Smart transformer control of the electrical grid

Giovanni De Carne[1], Marco Liserre[2] and Felix Wald[1]

This chapter introduces the smart transformer (ST) concept, a power electronics-based transformer that, in addition to the voltage transformation, can offer enhancing services to the grid. The chapter begins with a brief introduction on the ST concept and gives an overview of the offered services. In the second section, the ST architecture and control for each transformation stage are described, analyzing different topology alternatives. Basic and more advanced services provided to the grid are described in the third section that includes the innovative concept to regulate the grids power consumption by means of controlled voltage or frequency variations. The chapter closes with an overview of innovative grid concepts, such as DC grids.

13.1 The smart transformer concept

The first idea of a power electronics transformer (PET) can be found in 1968, when W. Mc Murray patented an idea of a DC transformer having a high frequency link [1]. The idea referred to the possibility to control the DC voltage under different amplitude outputs by means of solid-state switches and electronic controls. In the 1980*s*, Brook proposed an innovative transformer [2] where a "voltage shaping" capability of the DC transformer has been considered, moving the focus from the hardware configuration to the possible services that the PET could provide.

Despite an increasing attention to the topic, larger PET prototypes have only been realized since the beginning of the 2000′. The large-scale application of insulated-gate bipolar transistor (IGBT) first, and silicon carbide-/galium nitride-based Mosfets then allowed to reduce the PET's volume and weight, while increasing its efficiency. First examples of PET transformers were realized for traction applications, with the goal to increase the efficiency of the transformation stage, while reducing volume and weight [3,4]. Despite technically successful (the desired goals were achieved), the system was never put on the market, due to the restricted range of possible business cases.

[1]Institute for Technical Physics, Karlsruhe Institute of Technology, Germany
[2]Chair of Power Electronics, Kiel University, Germany

Only in recent years, the PET has been considered as an alternative for conventional transformers in medium-voltage (MV)/low-voltage (LV) substations. The need for power scalability, higher grid controllability, and availability of DC ports made the PET an interesting solution for grid operators. Several academic partners began to develop first prototypes for grid applications, such as the FREEDM center in US [5], focusing on demonstrating the PET performance in terms of efficiency and power routing capability for AC and DC microgrid applications [6].

Starting from the PET's advanced features, the HEART project, carried out at the Kiel University in Germany, has developed the ST concept [7,8]. The HEART project aims at demonstrating the advanced functionalities and the services that a ST can offer to the distribution grid.

To identify which possible services a ST is able to provide to the distribution grid, three different grid levels can be considered, all of them are shown in Figure 13.1: MV AC grid, LV AC grid, and DC grid (assumed as future grid scenario).

The MV AC/DC converter works as front-end converter for the MV grid, controlling the active power flow in order to keep the MV DC link voltage stable. As additional degree of freedom, the ST is able to regulate the injection of reactive

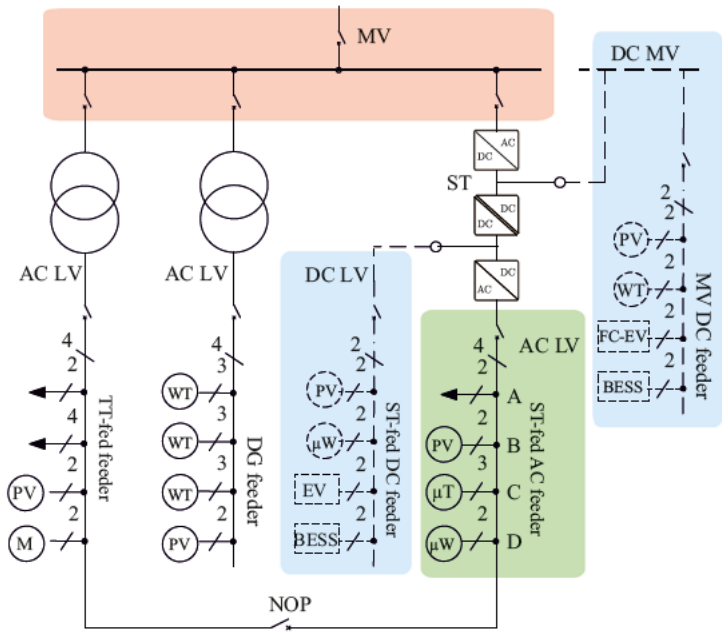

Figure 13.1 ST concept to provide services in distribution grids: load identification and control in LV grids (green area), active and reactive power support in MV grids (red area), enabled DC connectivity in MV and LV side (blue area)

power in the MV grid, and, at the same time, offer harmonic compensation capability. It can provide reactive power compensation services at the MV busbar level, offer voltage regulation support in the MV grid, and compensate the current and voltage harmonic content coming from large industrial loads (Figure 13.1 red box).

As mentioned above, the ST provides a first interface for AC grids with future DC grids (Figure 13.1, blue box). Depending on the architectures, this connection can be realized at both LV and MV levels. If realized at MV DC level, this connection can create a new concept of regional distribution systems, enabling the connection of MW-scale DC loads (e.g., electrolyzers, fast charging electric vehicle stations) or generators (e.g., photovoltaic, wind parks, and large size energy storage systems). In LV DC, small generators and loads, like electric vehicles and batteries, can be hosted. Due to a reduction in the power conversion AC/DC stages, the system losses can be reduced.

At the LV AC side, the ST works as stiff grid-forming converter, controlling the voltage waveform in the fed grid (Figure 13.1, green box). Due to this feature, the ST can offer both basic and advanced services: as an example of basic service, the ST shall provide always a three-phase balanced voltage independently from the current waveforms, that can be unbalanced or affected by harmonic content. An advanced service, that we are going to discuss in this chapter, is the capability to modify the power consumption of voltage- and frequency-dependent loads, acting on the voltage and frequency magnitude. This feature makes a variety of services possible, that are not available with conventional solutions (e.g., iron transformer): the on-line identification of the load power sensitivity to voltage and frequency variations; the voltage- and frequency-based load control to shape the power consumption, upwards and downwards, acting on a controlled variation of the voltage and frequency and on the load sensitivity to these variables; the provision of primary frequency regulation support, by adapting the load consumption depending on the measured MV frequency.

13.2 ST architectures and control

The ST interfaces three different grid topologies that vary on voltage levels as well as on supply system, either AC or DC (Figure 13.2): a MV AC grid, a LV AC grid, and two optional DC grids, both at MV and LV level (assumed as futuristic scenario). As a consequence, the ST three stage operations are interlaced: the MV converter controls the MV AC active current to regulate the MV DC link voltage at the nominal value. It can regulate the reactive power injection independently from the active power, remaining in the converter ampacity limits. The DC/DC converter transfers the power from the MV to the LV DC link in order to control the voltage in the LV DC link. The LV side converter controls the AC voltage waveform to be sinusoidal and balanced, and, upon request, it can shape the load consumption acting on voltage parameters (e.g., magnitude and frequency).

In the following sections, the topology and control of each stage has been described in detail, in order to give the reader a clear overview of the STs' features.

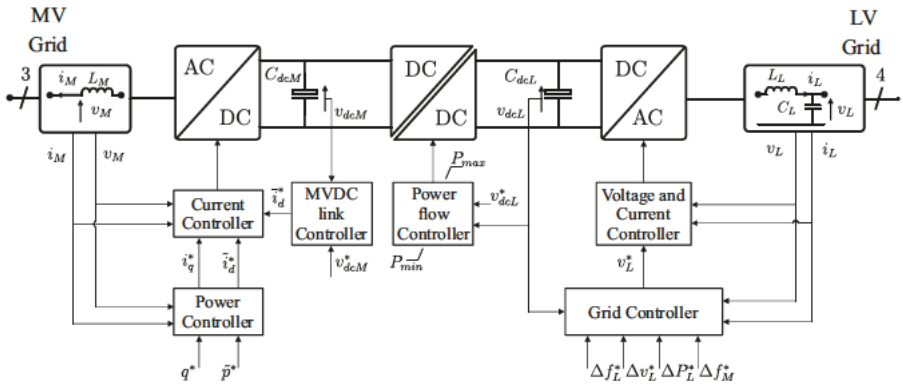

Figure 13.2 ST control overview

13.2.1 MV AC/DC converter

The ST MV stage interfaces the MV DC link to the MV AC grid. Depending on the countries, this stage works at relatively high voltage (> 10 kV), and due to the limited power for MV applications, at low current (< 100 A). This requirement led to investigate different topologies that can respect this high-voltage/low-current need. For these reasons, multi-level solutions have been considered for ST applications, and among the existing ones, good candidates are the one shown in Figure 13.3:

(a) *Neutral point clamped (NPC):* simple multi-level solution, largely adopted in industry, that provides DC-link access in the middle-point. As main drawback, the reduced number of levels implies large output filters and relatively high switching frequencies, increasing the losses.

(b) *Cascaded half-bridge (CHB):* modular design, low switching frequency, and low control complexity make the CHB a valid solution for ST. However, this topology does not provide direct access to the MV DC link (like the MMC) and it requires isolated DC supplies for each cell.

(c) *Modular multi-level converter (MMC):* the performance of the MMC is similar to the one of a CHB, with the addition of the availability of a MV DC link connection. On the down side, the MMC requires a more complex control structure and bulky DC capacitors.

At the MV stage, the ST control consists of two layers (Figure 13.2): in the first one, the MV DC link voltage and the AC current are regulated, while in the second one, grid services can be provided by means of a power controller (e.g., voltage support, power factor compensation, and active filtering). In the first layer, the MV DC link controller compiles the active current reference i^*_{dM} for the current controller (Figure 13.4), which is needed to maintain the DC voltage v_{dcM} at the nominal value. The ST current controller, absorbing the desired AC active current, is able to keep the DC link voltage constant, complying with the LV-side load energy request plus

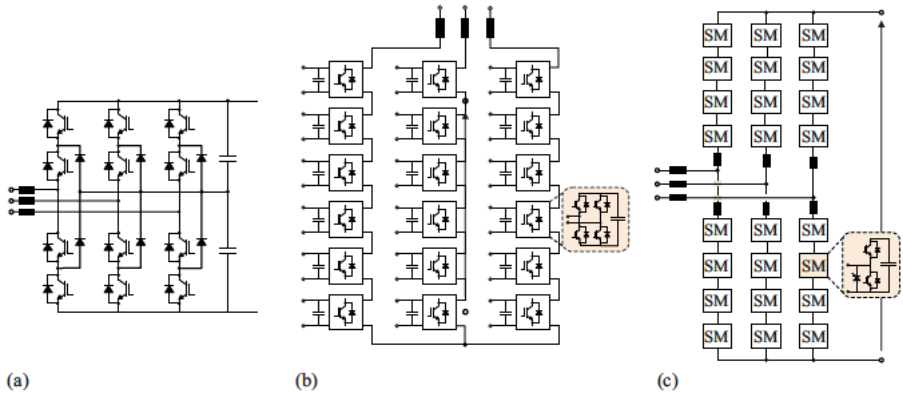

Figure 13.3 Common MV AC/DC converter topologies for a ST: (a) NPC converter, (b) CHB, and (c) MMC

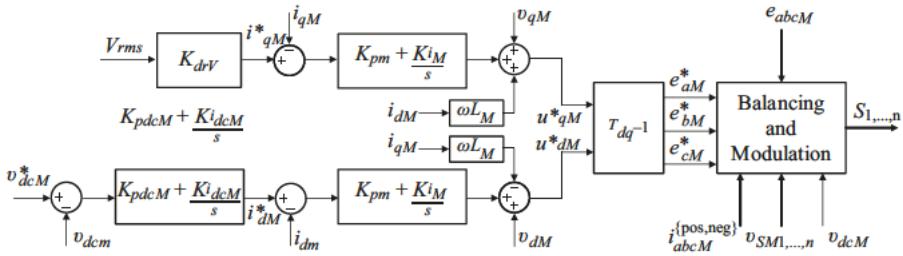

Figure 13.4 Generic ST MV AC/DC converter control structure in dq rotating framework

the ST losses. As shown in Figure 13.4, the power controller can provide both active and reactive power. As an example of this capability, the outer power loop controller can deliver reactive current (i_{qM}) depending on an external signal (e.g., the MV grid *rms* voltage V_{rms}) and the implemented control law (in this example a simple droop characteristic K_{drV}).

The internal control loop regulates the output current, minimizing the error between the current references coming from the power controllers i^*_{dM} and i^*_{qM}, and the measured grid currents i_{dM} and i_{qM}, respectively. The control output is then sent to a modulation block, which will create the new switching signals for the power semiconductors $S_{1,\ldots,N}$. Depending on the chosen topology (e.g., for CHB or MMC), additional balancing algorithms may be inserted in series or parallel to this control structure.

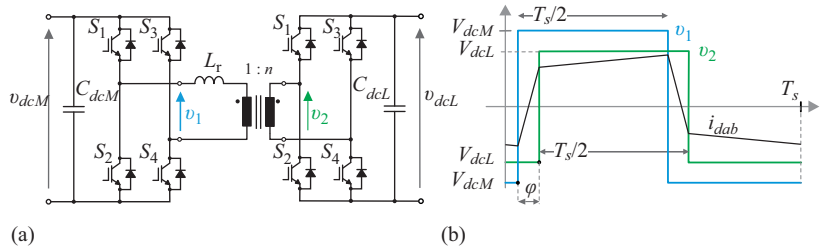

Figure 13.5 (a) Schematic circuit of a DAB and (b) voltages and currents at the primary and secondary side of DAB windings

13.2.2 DC/DC conversion stage

The ST can play a role in the future grid as enabler of DC distribution grids (Figure 13.1, blue box). The presence of a double DC link, at LV and MV level, offers a natural connection point for DC technologies. MV DC grids can in the future enable the direct connection of MW-scale DC loads or generators, like PV and wind parks, large size BESS and fast charging electric vehicle (FCEV) stations, without the need of additional AC/DC conversion stages. At LV level, DC grids provide a valid alternative to AC grids to integrate smaller generators and loads, like electric vehicles (EV) and battery energy storage systems (BESS), reducing the conversion losses caused by the additional AC/DC stages at the user side. These two DC stages are interfaced and controlled by means of a DC/DC converter that shall offer galvanic insulation, voltage transformation, and power flow controllability. The DC/DC converter technologies currently investigated for ST applications are the dual (or Multiple) active bridge (DAB) and series resonant converter (SRC).

(a) *DAB*: The DAB technology (Figure 13.5) regulates the power flow P_{dabL} between primary and secondary windings, acting on the primary v_{dcM} and secondary v_{dcL} voltage waveform phase shift ratio d:

$$P_{dabL} = \frac{v_{dcL} v_{dcM}}{2 N f_s L_r} d\,(1-d) \tag{13.1}$$

where N is the transformer turning ration, f_s is the DAB switching frequency, and L_r is the leakage inductance of the transformer. It follows that the power flow controller regulates the LV DC link voltage v_{dcL} at the nominal value, by controlling the power flow between the MV and LV DC link. The main advantage of this topology is the possibility to directly control the power flow and perform control strategies on the output voltage. As main drawback, the control complexity and losses are increased with respected to the SRC solution.

(b) *Series resonant converter (SRC)*: The SRC (Figure 13.6(a)) is an open-loop controlled DC/DC converter, that is based on a resonant tank for transferring energy

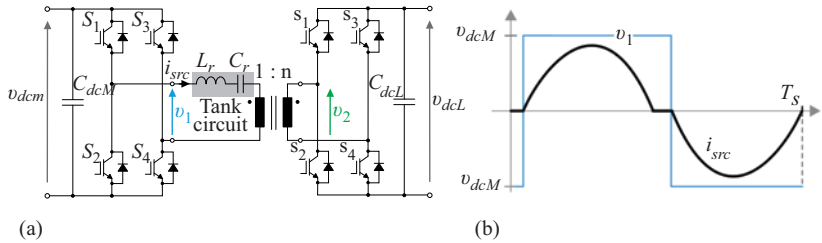

Figure 13.6 (a) Schematic circuit of an SRC and (b) voltages and currents at the primary side of an SRC

between the primary and the secondary winding. Effectively, the SRC works as a high-efficiency ideal DC transformer, transforming the DC voltage in open loop (i.e., without voltage feedback), as shown in Figure 13.6(b). The main advantage is the simplicity of the control solution and a lower need for measurements on the secondary side. On the other hand, it does not allow a power flow control, and for some topologies, bi-directional power flow.

13.2.3 LV DC/AC converter

The ST LV DC/AC stage synthesizes a balanced voltage waveform, working as grid forming converter for the LV grid. With respect to classical grid-forming converters for electric drive applications, the ST shall offer a neutral conductor return path, due to the presence of single-phase loads in the LV grid.

In order to offer the neutral conductor return path, several topologies, shown in Figure 13.7, have been considered for the ST LV side [9]:

(a) *NPC*: As described in the MV converter solutions, the NPC offers a multi-level solution, with the availability of the neutral path connection to the DC link mid-point.

(b) *Two-level Four-leg converter*: The classical two-level converter is the most common solution for LV applications, due to its simple control, low conduction losses, and low number of required switches. The main drawback is the need for a higher switching frequency in order to achieve a clean current output waveform.

(c) *Three-level T-type converter*: Offers the same control simplicity of the two-level converter, while it achieves an improved quality of voltage and low switching losses, typical of an NPC converter.

The voltage control in the ST grid is achieved by means of a cascaded voltage and current control loop. The control can be performed in static *abc*, $\alpha\beta$, or rotating *dq*0 frames. The advantage of using the *dq*0 rotating frame is the reduction of the control equations from 3 to 2 sets. However, this advantage is minimized in this case due to the presence of the neutral conductor connection that increases the number of independent phases. A possible control scheme is shown in Figure 13.8, where

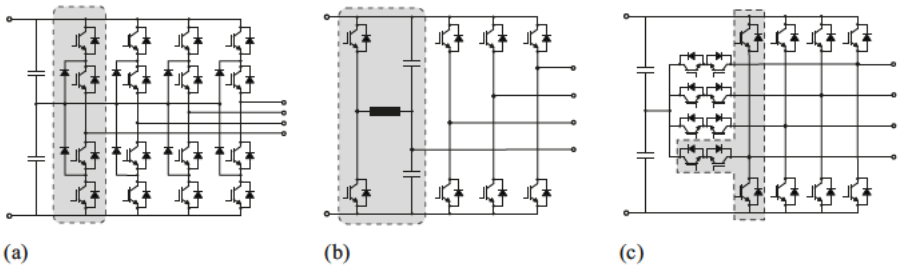

Figure 13.7 ST LV converter topologies: (a) NPC converter, (b) two-level four-leg converter, and (c) three-level T-type converter

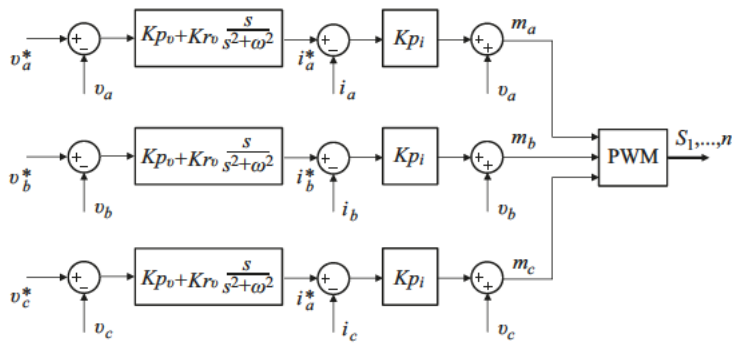

Figure 13.8 ST LV DC/AC converter controller scheme, example in an abc static reference frame

the voltage and current control loops are developed in *abc* static frame by means of proportional(-resonant) controllers. The voltage reference of each phase (e.g., v_a^*) is compared to the measured voltage, and their mismatch minimized, setting the new current reference i_a^*. An internal current loop is added normally, either with a simple gain (e.g., Kp_i in Figure 13.8) or with a resonant controller, to offer additional current damping.

13.3 Services provision to AC grids

A main property of the ST is the AC power flow decoupling between the MV and LV grids, thanks to the presence of one or more DC stages. This decoupling allows to control the two grids independently, with the only connection link represented by their energy exchange.

This section provides an overview of the services that the ST can offer to the AC grids thanks to the AC power flow decoupling property.

13.3.1 Disturbance rejection

Conventional transformers are characterized by a passive transformation of the voltage, independently from the power quality status. If a temporary LV condition or a voltage swell occurs in the MV grid, it is transferred to the LV grid. At the same time, if the LV grid load shows unbalanced or harmonic current absorption, its impact is seen also at the MV side. Thanks to the AC power flow decoupling capability, the ST is able to reject voltage or current disturbances from both primary and secondary sides, avoiding to transfer it to the other grid.

In Figure 13.9, several common disturbances at both low and medium voltage side have been considered, and the capacity of the ST of rejecting them has been depicted:

(a) *Voltage sag in MV grid:* during faults it may occur that the voltage drops below the normal operative conditions. In this case, the ST avoids to transfer the disturbance to the secondary side. However, as can be seen in the first column of Figure 13.9, the MV DC-link voltage drops sharply after the voltage drop. This is due to the need to deliver the required energy in the LV grid, while the available power in MV grid is reduced. After few cycles, the DC-link controller is able to restore the voltage at the nominal value.

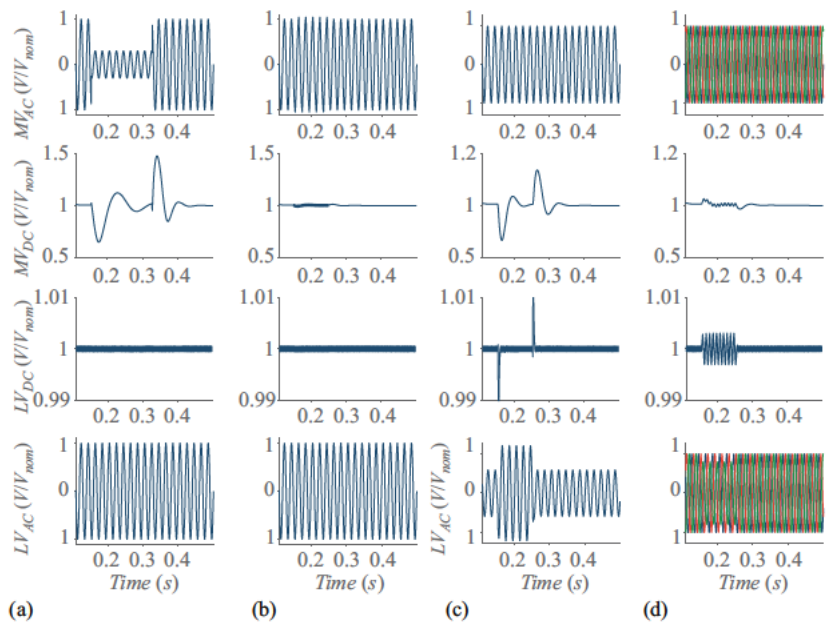

Figure 13.9 Voltages and/or currents of different stages for (a) a voltage sag on MV side, (b) harmonics on MV side, (c) load step on LV side, and (d) unbalanced loads on LV side

(b) *Harmonic voltage in MV grid:* large industrial loads can inject high harmonic currents, that can affect the grid voltage. In the second column of Figure 13.9, a 5th harmonic voltage of 5% has been inserted in the voltage waveform. As can be noticed, the LV grid voltage is perfectly sinusoidal, and only a fourth-order voltage ripple can be seen on the MV DC-link.

(c) *Load increase in LV grid:* fast power variations are common in LV grids, due to the sudden power decrease (e.g., after local faults, cloud passing on photovoltaic plants), or increase (e.g., during fast charging of electric vehicles). The ST is able to quickly damp the fast power change, leaving the MV grid voltage unaffected. As can be seen in the third column of Figure 13.9, the energy to cope with the sudden power increase is provided by the MV DC-link, while its controller restores the DC-link voltage after several tens of milliseconds.

(d) *Unbalanced load in LV grid:* due to the presence of single-phase loads, the LV grid power demand can be unbalanced. A conventional transformer tends to transfer such a unbalanced condition to the primary side, while the ST is able to appear as a perfectly balanced load at the primary side, as shown in the fourth column of Figure 13.9. As only effect, a second-order voltage oscillation can be noted in both MV and LV DC link, due to the 100 Hz power component in unbalanced load conditions.

13.3.2 Load sensitivity identification

Any control action involving the voltage or frequency [10,11], without a proper estimation of the loads active and reactive power response to voltage and frequency variations, can lead to incorrect control actions. A typical example of such a controller is the conservation voltage reduction (CVR) method [12,13]. Operating on the transformer tap-changer, the load power consumption can be decreased, achieving a relatively low-cost measure for energy-saving purposes.

In industrial practice, the load sensitivities to voltage and frequency variations are assumed *a priori*, using historical, statistical, or technical analysis, but they are not estimated in real time. If the real sensitivity changes during operation, any voltage- or frequency-based corrective action could under-perform.

To overcome this limitation, the on-line load identification approach has been developed in [14]. The approach applies an intentional small perturbation in voltage or frequency magnitude, while measuring the resulting load power variation. This enables the estimation of the load sensitivity in real time. Since only a small variation is necessary (i.e., about $1-2\,\%$) the experiment can be repeated as often as deemed necessary, e.g., every hour or every 10 min.

The load sensitivity to voltage and frequency expresses the variation in power consumption during a voltage amplitude and frequency change in the grid. The load power consumption depends on four parameters: voltage amplitude, frequency, time, and the initial operating point. The load power consumption can be mathematically generalized as follows:

$$\begin{aligned} P &= P(V, f, t, P_0) \\ Q &= Q(V, f, t, Q_0) \end{aligned} \tag{13.2}$$

where V and f are the voltage amplitude and the frequency, respectively; t represents the power dependency on the time, due to the capability of certain loads to restore their power in time (neglected in this analysis for matter of simplicity); P_0 and Q_0 are the initial operating conditions.

To represent the relation between voltage, frequency and measured power mathematically, the exponential model, described in (13.3), has been chosen:

$$\begin{aligned} P &= P_0 \left(\frac{V}{V_0}\right)^{K_p} \left(1 + K_{fp}\frac{f - f_0}{f_0}\right) \\ Q &= Q_0 \left(\frac{V}{V_0}\right)^{K_q} \left(1 + K_{fq}\frac{f - f_0}{f_0}\right) \end{aligned} \tag{13.3}$$

where K_p, K_{fp}, K_q, and K_{fq} are the active and reactive power sensitivity coefficients on voltage and frequency, respectively. Although any mathematical model (e.g., ZIP) can fit the sensitivity identification purpose, this model has been chosen due to the following characteristics [15]:

- It is independent of the initial voltage and it does not require initialization.
- Only one parameter identifies the relation between active and reactive power, voltage and frequency.
- The exponent is equal to the load sensitivity to the voltage.

Initially only the voltage sensitivities will be considered, assuming the grid frequency constant, the derivative of (13.3) with respect to V results in:

$$\begin{aligned} \frac{dP}{dV} &= K_p P_0 \left(\frac{V}{V_0}\right)^{K_p - 1} \frac{1}{V_0} \\ \frac{dQ}{dV} &= K_q Q_0 \left(\frac{V}{V_0}\right)^{K_q - 1} \frac{1}{V_0} \end{aligned} \tag{13.4}$$

and with the assumption of $V{=}V_0$, we obtain:

$$\begin{aligned} \frac{dP/P_0}{dV/V_0} &= K_p \\ \frac{dQ/Q_0}{dV/V_0} &= K_q \end{aligned} \tag{13.5}$$

Although the voltage reference V_0 is known (i.e., the nominal voltage), the variable P_0 in (13.5) depends on the nominal conditions, that are usually not met in normal

grid operations. However, in the case of exponential loads (13.3), the voltage base V_0 and P_0 can be chosen arbitrarily as any voltage V_1 and P_1:

$$\begin{aligned} \frac{P_1}{V_1^{K_p}} &= \frac{P_0}{V_0^{K_p}} \\ \frac{Q_1}{V_1^{K_q}} &= \frac{Q_0}{V_0^{K_q}} \end{aligned} \tag{13.6}$$

It follows that the active and reactive power sensitivities to voltage variations can be calculated independently from the *i*th operating point:

$$\begin{aligned} \frac{dP/P_i}{dV/V_i} &= K_p \\ \frac{dQ/Q_i}{dV/V_i} &= K_q \end{aligned} \tag{13.7}$$

Finally, (13.7) can be discretized for any time step t_k, where the chosen base is represented as previous time step t_{k-1}:

$$\begin{aligned} \frac{\frac{P(t_k)-P(t_{k-1})}{P(t_{k-1})}}{\frac{V(t_k)-V(t_{k-1})}{V(t_{k-1})}} &= K_p \\ \frac{\frac{Q(t_k)-Q(t_{k-1})}{Q(t_{k-1})}}{\frac{V(t_k)-V(t_{k-1})}{V(t_{k-1})}} &= K_q \end{aligned} \tag{13.8}$$

Similar to the voltage sensitivity coefficients, also the frequency sensitivity coefficients can be estimated considering the voltage at the nominal value $V = V_0$, so that (13.3) becomes:

$$\begin{aligned} P &= P_0 \left(1 + K_{fp}(f - f_0)\right) \\ Q &= Q_0 \left(1 + K_{fq}(f - f_0)\right) \end{aligned} \tag{13.9}$$

With respect to the voltage sensitivities case, now the relation between power and frequency is assumed linear. The frequency sensitivity of load power is computed as:

$$\begin{aligned} \frac{dP/P_0}{df} &= K_{fp} \\ \frac{dQ/Q_0}{df} &= K_{fq} \end{aligned} \tag{13.10}$$

Repeating the same steps as for the voltage sensitivity coefficients, and thus discretizing (13.10) at the time t_k, the frequency sensitivity coefficients can be estimated:

$$\begin{aligned} \frac{\frac{P(t_k)-P(t_{k-1})}{P(t_{k-1})}}{\frac{f(t_k)-f(t_{k-1})}{f_0}} &= K_{fp} \\ \frac{\frac{Q(t_k)-Q(t_{k-1})}{Q(t_{k-1})}}{\frac{f(t_k)-f(t_{k-1})}{f_0}} &= K_{fq} \end{aligned} \tag{13.11}$$

To estimate the load sensitivity to voltage and frequency in real conditions, the ST applies a controlled voltage (or frequency) disturbance in the grid. As an example of this disturbance, a trapezoidal profile has been adopted as controlled voltage variation, as shown in Figure 13.10 in a real measurement campaign performed at the Energy Smart Home Lab at the Karlsruhe Institute of Technology. The considered load is a common household, where different house appliances are connected at the same time, and the voltage is supplied by the LV DC/AC converter of the ST. As can be seen, the ST imposes a voltage variation and measures the load power consumption, in order to perform the calculation of the load dependence on the voltage mathematically. The trapezoidal shape used in this study varies the voltage amplitude of 0.02 pu for 0.4 s, with a voltage decreasing ramp equal to 0.05 pu/s. The choice of the disturbance characteristics, such as voltage amplitude and ramp-rate, comes from the compromise to limit the impact on the power quality in the grid (deep or long-lasting voltage variations) and to create a voltage variation that cannot be confused with the one caused by the stochastic load switching noise.

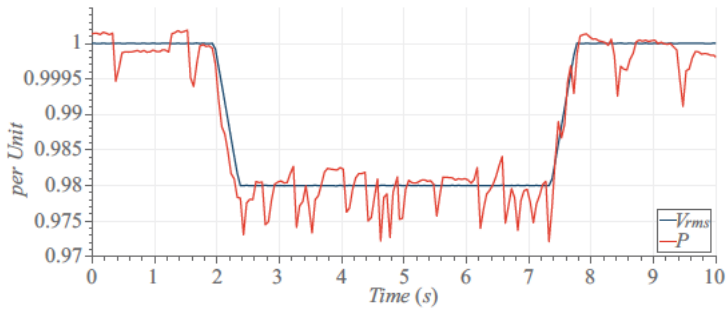

Figure 13.10 Example of an on-line load identification performed in a real experiment at the Energy Smart Home Lab at the Karlsruhe Institute of Technology. Measured load rms voltage and active power are plotted with a blue and red line, respectively.

13.3.3 Voltage-based load control

As demonstrated in the previous section, the ST is able to influence active power consumption of voltage-sensitive loads in a LV grid, by regulating the grid voltage amplitude. This section introduces a voltage-based load control [16] that, exploiting the voltage sensitivity coefficient estimation of the previous section, is able to achieve highly accurate load consumption variations.

Assuming that the LV grid is an unbalanced three-phase system with loads of different nature, each phase can have different load sensitivity coefficients. Let us consider that the load identification algorithm evaluates the voltage sensitivity coefficients K_p for each phase separately. To achieve this estimation, the ST introduces a controlled balanced three-phase voltage disturbance, that allows to measure the load power response in each phase independently. The total power variation ΔP for the three phases can be calculated as:

$$\Delta P = \Delta P_A + \Delta P_B + \Delta P_C \tag{13.12}$$

where P_A, P_B, P_C are the pre-disturbance consumed active powers for each phase, and ΔP_A, ΔP_B, ΔP_C are the corresponding phase load variations.

Let us consider the normalized load power sensitivity, as in (13.8) and let us apply the voltage-based load control to all three phases:

$$\begin{aligned}
\Delta P_A &= \frac{P_A}{V_A} K_{pA}(V - V_A) \\
\Delta P_B &= \frac{P_B}{V_B} K_{pB}(V - V_B) \\
\Delta P_C &= \frac{P_C}{V_C} K_{pC}(V - V_C)
\end{aligned} \tag{13.13}$$

Combining (13.13) and (13.12) and isolating the voltage which is applied for achieving a specified power variation ΔP, results in:

$$V = \frac{\Delta P + \left(P_A K_{pA} + P_B K_{pB} + P_C K_{pC}\right)}{\frac{P_A}{V_A} K_{pA} + \frac{P_B}{V_B} K_{pB} + \frac{P_C}{V_C} K_{pC}} \tag{13.14}$$

The ST main control feature allows to synthesize a balanced and sinusoidal three-phase set of voltages in the grid that are independent from the load current waveform demand (e.g., distorted or unbalanced). Under this assumption, let us simplify (13.14), imposing a voltage magnitude in each phase equal to the nominal one $V_A = V_B = V_C = V_0$.

It follows that the per-unit voltage amplitude V^*_{LV} that we have to impose to achieve the desired power change is defined with the formula:

$$\frac{V^*_{LV}}{V_0} = 1 + \frac{\Delta P}{P_A K_{pA} + P_B K_{pB} + P_C K_{pC}} \tag{13.15}$$

As can be noted from Figure 13.12, following a request to modify the connected load consumed active power ΔP, the ST applies a new voltage magnitude V_{LV}^{*} (Figure 13.11) that depends on the pre-calculated active power voltage sensitivity K_p. After an initial transient, the ST will restore the nominal voltage in the LV grid, in order to not impact on the load power quality for a long period.

An interesting application of the voltage-based load control is the support of primary frequency regulation to synchronous generators [17]. As shown in the example of Figure 13.13, the ST can measure the MV frequency f_{MV}, and it can adjust grid power ΔP following a certain characteristic:

$$\Delta P = \frac{1}{R_f}\Delta f_{MV} \tag{13.16}$$

controlling the LV amplitude V_{LV}, the load consumption of voltage-dependent loads P_{LV} varies depending on the direction and magnitude of the MV frequency variation. This service can provide power control instantaneously, and it is meant to provide

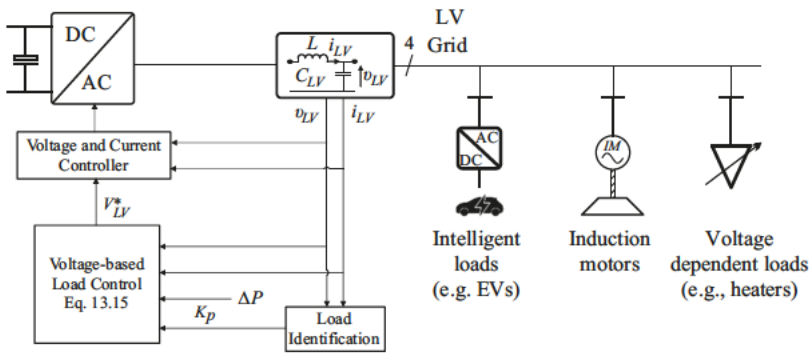

Figure 13.11 Voltage-based load control concept: interaction with intelligent loads, induction motors, and voltage-dependent loads (e.g., electric heaters)

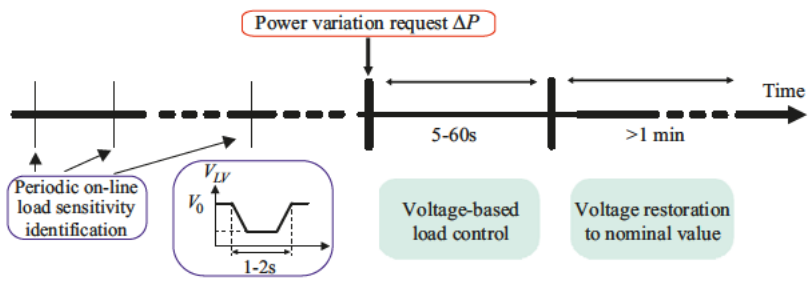

Figure 13.12 Timeline of the voltage-based load control actions

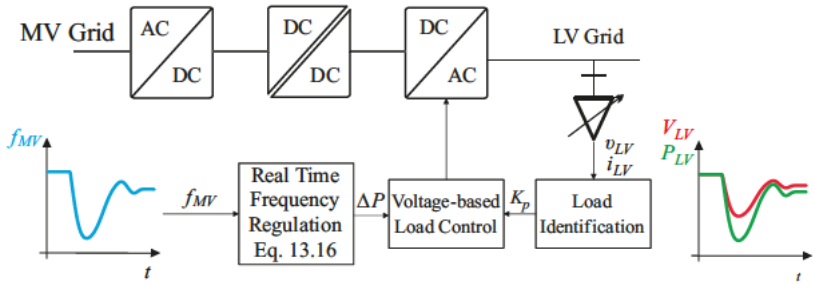

Figure 13.13 Real-time frequency regulation concept: blue line is the MV frequency f_{MV}; red line is the LV voltage amplitude V_{LV}; green line is the LV grid active power consumption P_{LV}

initial assistance to synchronous generators and larger energy storage systems (e.g., batteries) during their power ramp-up/-down. In a large-scale study in Ireland [18], it has been demonstrated that this feature can improve the system stability, while propelling the integration of wind turbines in the Irish system of an additional 10 %.

13.3.4 Frequency-based load control

In classical power system studies, the grid frequency is a variable that has to be kept constant in order to guarantee the stability of the system. This concept derives from the use of synchronous machines, which need a constant grid frequency.

However, the ST decouples the AC power flow between the primary and the secondary side, allowing an independent control of the frequency of the fed grid with respect to the main synchronous system. This possibility allows the use of controlled frequency variations as signals for local loads and generators to vary their consumption/production set-points.

Different appliances in AC systems are indeed equipped with power/frequency characteristics, in order to support the grid during power imbalances. Three common examples of these loads and generators can be found in Figure 13.14: an energy storage system used for example for photovoltaic applications, that can provide frequency regulation support to the grid; a synchronous machine, connected as example with a micro-gas turbine, that regulates the power output depending on the governor set-point; a domestic PV plant, equipped with derating power/frequency droop characteristic, if the grid frequency increases more than, e.g., in Germany, 50 Hz.

The ST can vary the secondary grid frequency in a controlled way, in order to vary the power set-point of the aforementioned energy resources, and thus regulate the fed grid net load [19]. Similar to (13.15), the frequency set-point f_{LV}^* can be decided with the frequency/active power sensitivity coefficients determined by (13.11):

$$\frac{f_{LV}^*}{f_0} = 1 + \frac{\Delta P}{P_A K_{pfA} + P_B K_{pfB} + P_C K_{pfC}} \tag{13.17}$$

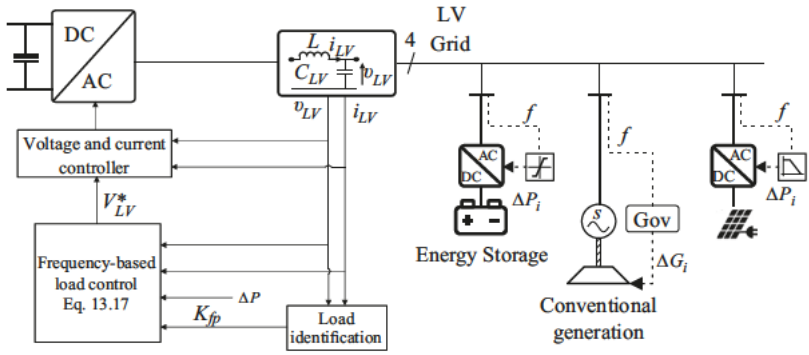

Figure 13.14 Frequency-based load control concept: interaction with energy storage systems, synchronous generators, distributed generator (e.g., PV plants)

This feature can extend the power controllability of the ST-connected load. As demonstrated in recent works, the frequency-based load control can be used, as an example, to avoid the reverse power flow in MV grid [19], or to avoid overloading a ST during high peak demand [20].

13.4 Enabling services for future DC grids

The ST offers a natural connection point for the future DC grids, where existing (e.g., photovoltaic) and new resources (e.g., energy storage systems and electric vehicle charging stations) can be integrated without additional AC/DC conversion stages [21,22].

A possible future grid architecture is shown in Figure 13.15, where the AC and the DC system co-exist. The resources, that by their nature work in DC, can decide to switch over to the DC grid, instead of remaining connected with the AC one, skipping a power transformation stage. A typical example is the charging of an electric vehicle: the AC connection can offer slow charging services (e.g., at home), reducing the size of the AC/DC converter, while the DC connection allows higher power capability, and thus more suitable for fast-charging (e.g., in public spots, such as commercial centers or offices).

In a future scenario, the loads can share both an AC and a DC connection (as shown in Figure 13.15) and re-route their power flow depending on efficiency reasons or grid needs. In [23], efficiency improvements up to 6 % and line losses reduction up to 22 % have been achieved using this grid topology.

As mentioned before, a DC connection can be realized directly from the ST conversion stages. At this regard, Figure 13.16 introduces two different architecture approaches to create a DC connection for LV grids [24]:

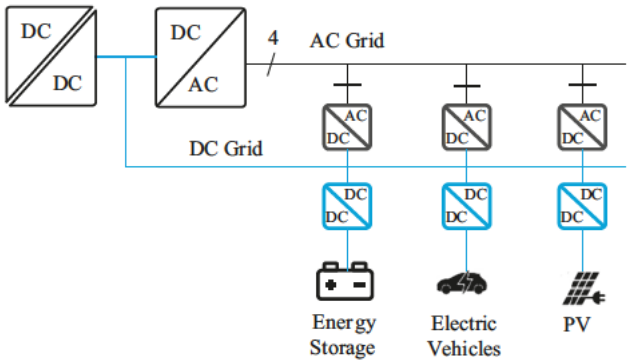

Figure 13.15 Hybrid DC/AC grid concept: the existing AC grid (black line) runs in parallel with the DC grid (blue line), allowing different connection possibilities to DC loads and generators

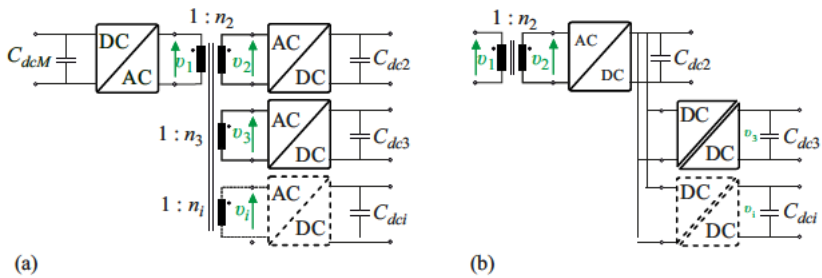

Figure 13.16 DC ports architecture: (a) magnetic coupling and (b) galvanic coupling

(a) *Magnetic connection*, where the medium frequency isolation transformer is realized with additional windings directly connected to the main transformer core. The power transfer does not occur at DC link level, but directly in the magnetic coupling. Despite a more complex transformer design, this architecture allows to reduce the number of semiconductor switches, decreasing the overall costs. With this topology, the number of DC ports is pre-determined at design level, and they cannot be scaled up.

(b) *Galvanic connection*, where the DC grid is directly connected to the ST LV DC link by means of a DC/DC converter. It allows great flexibility in adapting the voltage at different levels, and to scale up the number of DC connection ports. The downside is that for each new connection port, an isolated DC/DC converter is needed for voltage safety reasons.

13.5 Conclusions and future outlook

The ST, as a power electronics-based transformer, can increase the system controllability and offer services to the distribution grid. This chapter has provided an overview of the ST hardware and control features. It has introduced a new concept of estimating the load sensitivity to voltage and frequency, and how this information can be used to control the load consumption by means of controlled voltage and frequency variations. This chapter also described future DC grid scenarios based on ST, highlighting how a hybrid AC/DC distribution system can lower grid losses and improve system efficiency.

The ST topic is still at the beginning. More work is needed to integrate this technology into the distribution grid:

- Standards for asynchronously connected grids (i.e., the ST secondary side) shall be developed in order to integrate the ST safely into distribution grids.
- Business cases shall be proposed, in order to make the ST an attractive solution for distribution system operators and network utilities.
- Hardware efficiency shall be increased, that, despite the recent improvements in the switching technology, is still not at the same level of the conventional iron transformer.
- New control strategies shall be introduced, in order to fully exploit the increased power controllability of the ST.

Acknowledgment

The work of Giovanni De Carne and Felix Wald was supported by the Helmholtz Association and the Helmholtz Young Investigator Group under the program "Energy System Design" and "Hybrid Networks" (VH-NG-1613), respectively. The work of Marco Liserre has been supported by the German Federal Ministry of Education and Research (BMBF) within the Kopernikus Project ENSURE "New ENergy grid StructURes for the German Energiewende" under Grant 03SFK1I0-2.

Bibliography

[1] W. Mcmurray. Power converter circuits having a high frequency link, 1968, Patent, US3517300A.

[2] J.L. Brook, R.I. Staab, J.C. Bowers, and H.A. Niehaus. Solid state regulated power transformer with waveform conditioning capability, 1980, Patent, US4347474A.

[3] D. Dujic, A. Mester, T. Chaudhuri, A. Coccia, F. Canales, and J.K. Steinke. Laboratory scale prototype of a power electronic transformer for traction applications. In *Proceedings of the 2011 14th European Conference on Power Electronics and Applications*, Aug 2011, pp. 1–10.

[4] J.E. Huber and J.W. Kolar. Volume/weight/cost comparison of a 1mva 10 kv/400 v solid-state against a conventional low-frequency distribution transformer. In *2014 IEEE Energy Conversion Congress and Exposition (ECCE)*, Sept 2014, pp. 4545–4552.

[5] A.Q. Huang, M.L. Crow, G.T. Heydt, J.P. Zheng, and S.J. Dale. The future renewable electric energy delivery and management (freedm) system: the energy internet. *Proceedings of the IEEE*, 99(1):133–148, 2011.

[6] X. She, X. Yu, F. Wang, and A.Q. Huang. Design and demonstration of a 3.6-kv: 120-v/10-kva solid-state transformer for smart grid application. *IEEE Transactions on Power Electronics*, 29(8):3982–3996, 2014.

[7] M. Liserre, G. Buticchi, M. Andresen, G. De Carne, L.F. Costa, and Z.-X. Zou. The smart transformer: impact on the electric grid and technology challenges. *IEEE Industrial Electronics Magazine*, 10(2):46–58, 2016.

[8] L.F. Costa, G. De Carne, G. Buticchi, and M. Liserre. The smart transformer: a solid-state transformer tailored to provide ancillary services to the distribution grid. *IEEE Power Electronics Magazine*, 4(2):56–67, 2017.

[9] M. Schweizer and J.W. Kolar. Design and implementation of a highly efficient three-level t-type converter for low-voltage applications. *IEEE Transactions on Power Electronics*, 28(2):899–907, 2013.

[10] P. Aristidou, G. Valverde, and T. Van Cutsem. Contribution of distribution network control to voltage stability: a case study. *IEEE Transactions on Smart Grid*, PP(99):1–1, 2015.

[11] G. Delille, B. Francois, and G. Malarange. Dynamic frequency control support by energy storage to reduce the impact of wind and solar generation on isolated power system's inertia. *IEEE Transactions on Sustainable Energy*, 3(4): 931–939, 2012.

[12] K.P. Schneider, J. Fuller, F. Tuffner, and R. Singh. Evaluation of conservation voltage reduction (cvr) on a national level. *Pacific Northwest National Laboratory Report*, 2010.

[13] Z. Wang and J. Wang. Review on implementation and assessment of conservation voltage reduction. *IEEE Transactions on Power Systems*, 29(3): 1306–1315, 2014.

[14] G. De Carne, M. Liserre, and C. Vournas. On-line load sensitivity identification in lv distribution grids. *IEEE Transactions on Power Systems*, 32(2): 1570–1571, 2017.

[15] T. Van Cutsem and C. Vournas. *Voltage Stability of Electric Power Systems*. Kluwer Academic Publishers, Amsterdam, 1998.

[16] G. De Carne, G. Buticchi, M. Liserre, and C. Vournas. Load control using sensitivity identification by means of smart transformer. *IEEE Transactions on Smart Grid*, 9(4):2606–2615, 2018.

[17] G. De Carne, G. Buticchi, M. Liserre, and C. Vournas. Real-time primary frequency regulation using load power control by smart transformers. *IEEE Transactions on Smart Grid*, 10(5):5630–5639, 2019.

[18] J. Chen, M. Liu, G. De Carne, *et al*. Impact of smart transformer voltage and frequency support in a high renewable penetration system. *Electric Power Systems Research*, 190:106836, 2021.

[19] G. De Carne, G. Buticchi, Z. Zou, and M. Liserre. Reverse power flow control in a st-fed distribution grid. *IEEE Transactions on Smart Grid*, 9(4): 3811–3819, 2018.

[20] G. De Carne, G. Buticchi, M. Liserre, and C. Vournas. Frequency-based overload control of smart transformers. In *2015 IEEE Eindhoven PowerTech*, 2015, pp. 1–5.

[21] X. She, A.Q. Huang, S. Lukic, and M.E. Baran. On integration of solid-state transformer with zonal dc microgrid. *IEEE Transactions on Smart Grid*, 3(2):975–985, 2012.

[22] X. Yu, X. She, X. Zhou, and A.Q. Huang. Power management for dc microgrid enabled by solid-state transformer. *IEEE Transactions on Smart Grid*, 5(2):954–965, 2014.

[23] D. Das, V.M. Hrishikesan, C. Kumar, and M. Liserre. Smart transformer-enabled meshed hybrid distribution grid. *IEEE Transactions on Industrial Electronics*, 68(1):282–292, 2021.

[24] L.F. Costa, G. Buticchi, and M. Liserre. Optimum design of a multiple-active-bridge dc–dc converter for smart transformer. *IEEE Transactions on Power Electronics*, 33(12):10112–10121, 2018.